CrystEngComm

PAPER

View Article Online
View Journal | View Issue

Cite this: *CrystEngComm*, 2015, **17**, 422

Location of CO_2 during its uptake by the flexible porous metal–organic framework MIL-53(Fe): a high resolution powder X-ray diffraction study†

Nathalie Guillou,[a] Sandrine Bourrelly,[b] Philip L. Llewellyn,[b] Richard I. Walton*[c] and Franck Millange*[a]

Received 7th July 2014,
Accepted 4th September 2014

DOI: 10.1039/c4ce01393j

www.rsc.org/crystengcomm

The interaction of CO_2 with the porous metal–organic framework material MIL-53(Fe), $Fe^{III}(OH)_{0.8}F_{0.2}[O_2C–C_6H_4–CO_2]$ has been studied by complementary gas adsorption and high resolution powder X-ray diffraction as a function of gas pressure. It has been shown that CO_2 adsorption occurs in three steps, with firstly the formation of an "Intermediate" (INT) form [S. G. $P\bar{1}$; V = 916.80(6) Å^3] at room temperature and 2 bar, followed by the transition to a "Narrow Pore" (NP) form [S. G. *C*2/*c*; V = 1083.01(2) Å^3] at 10 bar. The "Large Pore" (LP) form [S. G. *Imcm*; V = 1563.10(4) Å^3] is obtained also at 10 bar but by decreasing the temperature to 220 K. Crystal structures of the three CO_2 materials MIL-53(Fe)[nCO_2], with n = 0.22, 0.63 and 2.72, have been solved and refined, which has allowed precise localisation of guest CO_2 molecules, not previously determined. This shows that the (INT) form presents two types of tunnels of different sizes, with only the largest ones are occupied by the CO_2 molecules. In the (NP) and (LP) forms, all tunnels become equivalent and are occupied by CO_2. The huge unit cell volume increase of the (LP) form leads to drastic increase in the amount of CO_2 adsorbed. In the three forms, CO_2 molecules are located in order to favour interactions between their oxygen atoms and the OH/F groups of the framework and there is no evidence for guest–guest interactions until the highest loading where short contacts of a similar distance found in solid CO_2 are observed.

1. Introduction

Porous metal organic frameworks (MOFs) are presently attracting much attention for applications as adsorbents for a variety of guest molecules, in particular for molecular separation and storage of gases such as CO_2, CH_4 and H_2 for environmental and energy reasons, but also of much larger molecules, typically encountered in the liquid phase, ranging from simple hydrocarbons to complex drug molecules.[1] In terms of CO_2 adsorption the goal of this research is often the capture and storage of large volumes of the gas at close to ambient conditions. In real situations CO_2 must often be captured in competition with other potential adsorbate molecules, such as water, sulfur and nitrogen oxides or hydrocarbons, for example, where combustion exhaust gases are being processed. Recent progress in CO_2 capture by MOFs has been the subject of several extensive review articles,[2] to which the reader is referred. It is clear from this work that diverse methods are being explored to optimise CO_2 binding in MOFs, such as inclusion of open metal sites,[3] engineering of ligand defects,[4] post synthesis partial exchange of metal ions,[5] in addition to the use of constricted pores (molecular sieving) familiar from zeolite science.[6]

One interesting strategy in the field of adsorption by porous MOFs is to make use of so-called breathing frameworks whose structure is able to respond to an external stimulus whilst overall connectivity of the structure is maintained.[7,8] Such materials have adaptable porosity depending on gas pressure and temperature, for example, which may allow the development of smart porous materials whose structure can respond to conditions of use. Materials with the MIL-53 structure are among the most well-studied examples of breathing MOFs: the structure undergoes a large and reversible structural swelling depending on the presence or absence of guest molecules, an effect which may also be brought about by temperature or pressure.[8,9] MIL-53 materials have an anisotropic, three-dimensional structure, being constructed from infinite inorganic chains (*trans*-corner shared M^{3+}-centred octahedra), cross-linked in two dimensions by the bidentate 1,4-benzenedicarboxylate ligand to give

---

[a] *Institut Lavoisier Versailles, Université de Versailles, UMR 8180, 78035 Versailles, France. E-mail: franck.millange@uvsq.fr*
[b] *Aix-Marseille University, Laboratoire MADIREL, UMR CNRS 7246, Centre de St Jérôme, 13397 Marseille Cedex 20, France*
[c] *Department of Chemistry, University of Warwick, Coventry, CV4 7AL, UK. E-mail: r.i.walton@warwick.ac.uk*

† Electronic supplementary information (ESI) available: Crystal structure data in cif format. See 10.1039/c4ce01393j

diamond-shaped channels. The trivalent metal in the prototype material may be any one of Cr, Al, Fe, V, Ga, In, Sc, and mixed-metal variants are also known.[10] Although some previous studies of CO_2 uptake in MIL-53 materials have been reported,[11–13] the precise location of the adsorbate as a function of loading has not been determined in most cases. This is largely due to the fact that the materials are only available as polycrystalline samples and structure solution from powder diffraction with large-volume unit cells is not necessarily straightforward; furthermore crystallographic characterisation requires long-range order of guest molecules, which may not always occur in the dynamic conditions of gas adsorption. In this paper we present a study of CO_2 uptake by MIL-53(Fe) in which we use knowledge gained from gas adsorption studies to interpret high-resolution powder X-ray diffraction patterns from samples loaded *in situ* with CO_2. The use of high-resolution synchrotron X-ray powder diffraction has the allowed a full structure solution and refinement of the host–guest materials, providing accurate information about the location of the CO_2 guest molecules in this archetypical MOF material.

2. Experimental section

2.1. Synthesis

MIL-53(Fe)[H_2O] was synthesised as reported in previous work.[14] The advantage of the fluorinated sample over its non-fluorinated analogue is its superior crystallinity for this fundamental study. MIL-53(Fe)[DMF] was first isolated as a pure-phase pale orange crystalline powder under reflux conditions (set at 423 K for 12 hours) from equimolar amounts of iron(III) chloride hydrate, $FeCl_3 \cdot xH_2O$ (Aldrich, 97%), 1,4-benzenedicarboxylic acid, $HO_2C–(C_6H_4)–CO_2H$ (Alfa 97%), hydrofluoric acid, HF (Prolabo, 40% in water) in excess *N*,*N*-dimethylformamide (DMF, Aldrich 99%). The light orange MIL-53(Fe)[MeOH] powder was obtained after dispersion of the as-synthesised material (which contains solvent) into methanol to remove the DMF guest molecules from the pores. Exchange with water was then performed to finally obtain the hydrated form MIL-53(Fe)[H_2O]. Quantitative elemental analyses (performed using ICP-MES for Fe, Schöniger flask combustion followed by titration for fluorine and by combustion analysis for CHN, by Medac Ltd., U.K.) gave the following results: Fe: 23.7%; C: 35.6%; H: 2.68% and F: 1.31% which compares well with the composition calculated from the formula $Fe^{III}(OH)_{0.8}F_{0.2}[O_2C–C_6H_4–CO_2] \cdot H_2O$: Fe: 21.9%; C: 37.6%; H: 2.68% and F: 1.48%, bearing in mind that surface termination by organics and the presence of a small amount of solvent will increase the carbon content, and that the analysis for fluorine in the presence of oxygen gives inherent errors in analysis.

2.2. Powder X-ray diffraction

Powder X-ray diffraction data were collected on ID31 at the European Synchrotron Radiation Facility (ESRF). The beamline receives X-rays from the synchrotron source (which operates with an average energy of about 6 GeV) from an undulator device. The incident X-ray wavelength was 0.79984 Å using an incident beam size of 2.0 mm (horizontal) × 1.0 mm (vertical). A powdered sample was contained in 1 mm diameter quartz capillary directly connected to an in-house built gas dosing system.[15] This equipment does not allow rapid sample spinning during data collection; nevertheless the sample can be oscillated over an angular range of approximately 120° to ensure better powder averaging. Prior to the measurements, the sample was outgassed under 10^{-3} mbar at 473 K for several hours. The activated sample [named "Closed Pore" (CP) form] was brought back to room temperature and successive doses of CO_2 were then introduced. A large number of scans were collected over the range of pressure (0–10 bars) and temperature (RT–220 K) to assess the various distinct phases present. Since our aim was to refine accurately the structures of these distinct structures, and the location of CO_2 within, we focussed on measuring the three different phases we observed. After a delay of one hour at each of these points, to be sure that no structural evolution was observed during that time, the powder data of each phase was measured precisely (6–8 hours data collection over the 2θ range 2–45°) to ensure the pattern was of sufficient quality for structure solution and refinement. Extraction of the peak positions, patterns indexing, direct space strategy used to complete the structural models, difference Fourier maps and Rietveld refinements were carried out with the TOPAS program.[16] For all three forms, unit cells and possible space groups were found by the LSI-Indexing method with satisfactory figures of merit (see Table 1).

2.3. Adsorption isotherms and microcalorimetry

Adsorption experiments at 303 K were carried out up to 55 bars using a commercial gravimetric adsorption device (Rubotherm Präzisionsmeßtechnik GmbH).[17,18] A step by step gas introduction mode was used. Prior to each experiment, the sample was outgassed at 523 K for 16 hours. Equilibrium was assumed when the variation of weight remained below 0.03% for 20 minutes. The adsorption isotherm obtained at 230 K was obtained with a commercial volumetric apparatus (Omnisorp 100, Coulter) which was adapted to use a helium cryostat allowing experiments to be carried out to 1 bar in the temperature range from 30 K to 300 K. To complete the adsorption isotherm data with energetic information, a manometric adsorption apparatus coupled with a Tian-Calvet type microcalorimeter was used.[19] This apparatus measures the isotherm and the enthalpy of adsorption simultaneously using a point by point introduction of gas to the sample. Prior to each adsorption experiment, the samples were outgassed at 423 K under a vacuum of 10^{-3} mbar. The CO_2 was obtained from Air Liquide (Alphagaz, France) of minimum purity N48 (minimum 99.998% depending on the gas). Each experiment was repeated several times, and both isotherms and enthalpy values at low coverage were obtained by averaging over all the experiments.

Table 1 Unit cell data and goodness of fit parameters for the MIL-53(Fe)[nCO$_2$] materials studied resulting from the Rietveld refinements

	"Intermediate" (INT) MIL-53(Fe)[0.22CO$_2$]	"Narrow Pore" (NP) MIL-53(Fe)[0.63CO$_2$]	"Large Pore" (LP) MIL-53(Fe)[2.72CO$_2$]
$n_{\max}$	0.25	1	3
S. G.	$P\bar{1}$	$C2/c$	$Imcm$
a/Å	6.8722(2)	20.8595(2)	16.5679(2)
b/Å	11.1022(4)	8.2508(1)	13.6384(3)
c/Å	13.9274(4)	6.8738(1)	6.91760(5)
α/°	108.314(2)	—	—
β/°	92.603(3)	113.7310(8)	—
γ/°	112.299(4)	—	—
V/Å^3	916.80(6)	1083.01(2)	1563.10(4)
Z	4	4	4
M_{20}	42	172	166
N_{ref}	1721	517	432
Structural parameters	45	19	19
R_B	0.031	0.042	0.070
R_{WP}, R_P	0.078, 0.059	0.088, 0.062	0.104, 0.072

3. Results and discussion

3.1. CO$_2$ adsorption and microcalorimetry

The behaviour of MIL-53(Fe) towards carbon dioxide was probed under various conditions of temperature and pressure (see Fig. 1 and 2). The isotherms show two general plateau regions. A first plateau is observed for an uptake of around 1.3 mmol g^{-1} ($\approx$ 0.3 mol$_{\text{CO}_2}$/mol$_{\text{MIL-53(Fe)}}$) whose length depends on the temperature region explored. Indeed, at 195 K this region seems to be a shoulder in the isotherm whereas this plateau is stable in the region 0.05–0.3 bar at 230 K and in the region 0.1–4.5 bars at 303 K. This is then followed by a second step and 'plateau' which is seen to vary in the region 3.2 ($\approx$ 0.8 mol$_{\text{CO}_2}$/mol$_{\text{MIL-53(Fe)}}$) to almost 4 mmol g^{-1} ($\approx$ 1 mol$_{\text{CO}_2}$/mol$_{\text{MIL-53(Fe)}}$) depending on temperature and pressure. A Van't Hoff plot following the position of this step with pressure (see Fig. 1b) shows a straight line region whose slope can be used to deduce energy. Here, this energy is estimated at 19 kJ mol^{-1}, which compares well to the experimentally observed enthalpy of 17 kJ mol^{-1} (see below). The amount adsorbed after this second step corresponds well to the uptake observed in the NP structures of MIL-53(Al) and MIL-53(Cr).[20] In the high pressure experiment, an upswing in the isotherm can be observed which suggests the formation of a third plateau. However with the equipment at our disposition it was not possible to reach higher pressures.

The adsorption enthalpies are shown in Fig. 2b. Two main enthalpy regions can be distinguished which can be associated with the two filling regimes. For the first filling region, an enthalpy of around 42 kJ mol^{-1} is measured; however enthalpies in the region of the enthalpy of liquefaction (17 kJ mol^{-1}) are measured during the second filling step. It is interesting to compare these results with those previously obtained with the MIL-53(Cr) and MIL-53(Al) structures.[20,21] Indeed, the energies of adsorption in the NP form of these structures is estimated in the region of 41 kJ mol^{-1} in the aluminium solid and 45 kJ mol^{-1} in the chromium solid. In this work, such energies are associated with the filling of the INT structure (see below), in which half of the pores have the same opening as the NP form. Interesting though, lower energies are associated with the filling of the NP structure of MIL-53(Fe) (17 kJ mol^{-1}) and this is more probably associated with the energy equally required to transform the structures from the INT to NP form. This behaviour is observed during the NP → LP transition in both MIL-53(Al) and MIL-53(Cr) and was again associated with the energy required for the structural transition.

3.2. CO$_2$ localization by X-ray powder diffraction

As previously observed,[11] the host MIL-53(Fe) undergoes structural swelling depending on the applied CO$_2$ pressure. Starting from the "Closed Pore" (CP) form, three different phases can be observed (see Fig. 3). At room temperature and a pressure around 2 bar, corresponding to the middle of the first plateau seen in the adsorption isotherm, the "Intermediate" (INT) form was isolated. When reaching 10 bar at room temperature, a "Narrow Pore" (NP) form of the MIL-53(Fe)[nCO$_2$] can be obtained, while maintaining the pressure at 10 bar and decreasing the temperature down to 220 K, the fully open "Large Pore" (LP) form was successfully isolated. Indexing of the three powder patterns [(INT), (NP) and (LP)] shows similarities with the unit cells previously reported for MIL-53(Fe)_int,[22] MIL-53(Fe)[H$_2$O] (ref. 23) and MIL-53(Fe)[2,6-lutidine,H$_2$O].[14] That led us to use directly the atomic coordinates of the frameworks of these three MIL-53 materials as starting models in the Rietveld refinements of the CO$_2$-loaded structures. At this stage, R_B and R_{wp} factors reached the following values for the (INT), (NP) and (LP) forms, respectively (R_B = 0.058/R_{WP} = 0.109, R_B = 0.051/R_{WP} = 0.096 and R_B = 0.158/R_{WP} = 0.191). The CO$_2$ guest molecules were then localised by both difference Fourier map calculations and a direct space approach based on simulated annealing. During Rietveld refinements, 1,4-benzenedicarboxylate ions were treated as rigid bodies along with the CO$_2$ molecules. The anisotropic line broadening effect was modelled by using

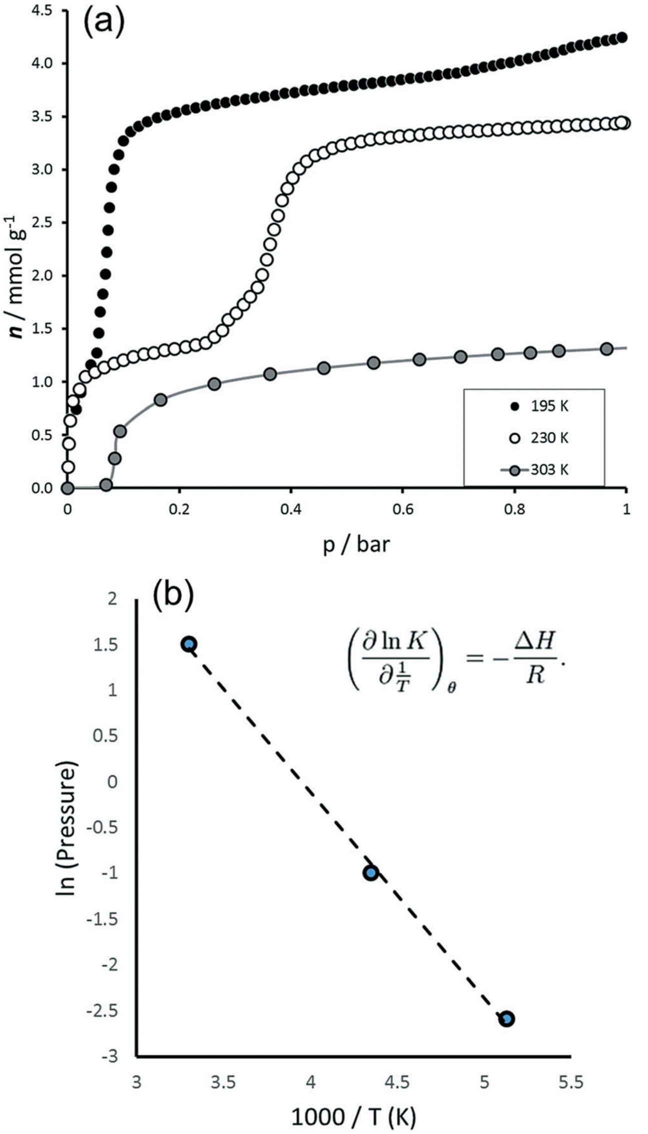

Fig. 1 Adsorption of CO_2 on MIL-53(Fe) to 1 bar. (a) Isotherms to 1 bar at 195 K, 230 K and 303 K. (b) Van't Hoff plot.

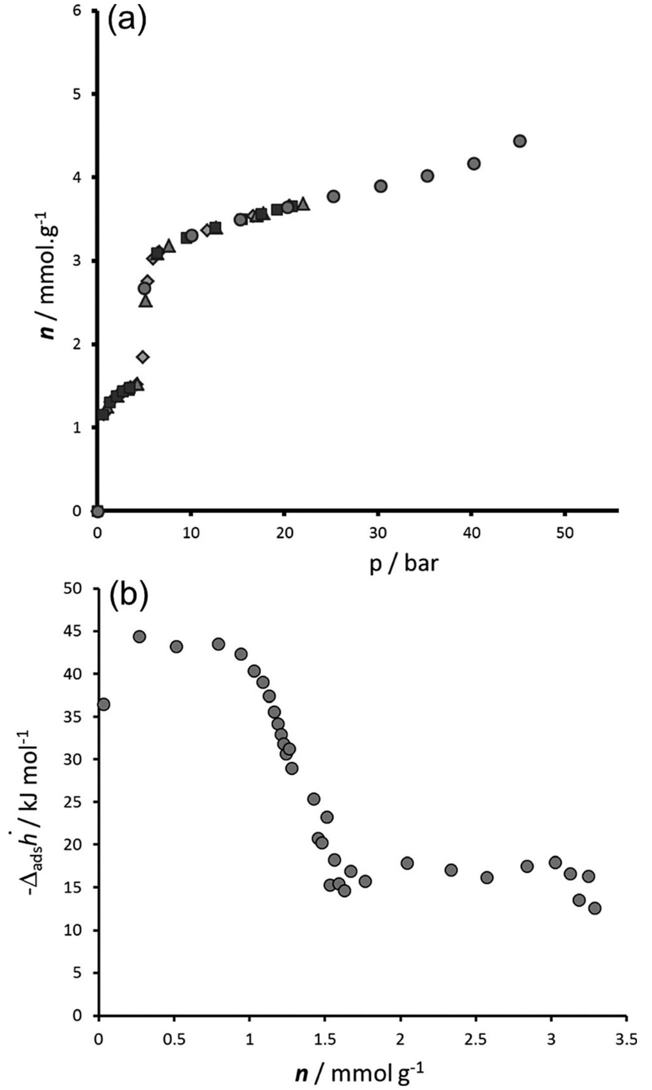

Fig. 2 Adsorption of CO_2 on MIL-53(Fe) at 303 K. (a) Isotherm repeated 5 times. (b) Enthalpies measured by calorimetry.

spherical harmonics series. The final Rietveld refinements gave satisfactory crystal structure model indicators and profile factors (see Table 1). It should be noticed that the (LP) form was not obtained as a pure phase under the working conditions (T = 220 K, P = 10 bars) since this one coexists with the (NP) form, whose amount was estimated (from quantitative analysis using the Rietveld method) at only 2.56(4)% in weight. The thermal factor of CO_2 molecules was arbitrarily fixed to 4 Å^2 in the three structural models and it is clear that the errors on occupancy factors of guest molecules are underestimated. For the three filling states, the CO_2/Fe ratio was refined and converged to a value of 0.22, 0.63 and 2.72 for the (INT), (NP) and (LP) form, respectively. The corresponding chemical formulae are therefore $Fe^{III}(OH)_{0.8}F_{0.2}[O_2C–C_6H_4–CO_2]·0.22CO_2$ for (INT), $Fe^{III}(OH)_{0.8}F_{0.2}[O_2C–C_6H_4–CO_2]·0.63CO_2$ for (NP) and $Fe^{III}(OH)_{0.8}F_{0.2}[O_2C–C_6H_4–CO_2]·2.72CO_2$ for (LP). These are written below using the notation MIL-53(Fe)[$n$$CO_2$] to be consistent with our earlier notation of MIL-53(M)[guest] materials.[14]

The filling of the pores by the CO_2 guest molecules leads to three different structures depending on pressure, for which the topology of the MOF skeleton is identical. The (INT) form crystallises in a triclinic unit cell (see Table 1). The crystallographic asymmetric unit contains two independent iron atoms and two OH/F groups on general positions, three carboxylate moieties [two on symmetry centres and one on general position] and one CO_2 molecule also localised on a symmetry centre [occupancy of 0.881(6)]. As already observed in the metastable phase MIL-53(Fe)_int obtained during the dehydration of the MIL-53(Fe)[H_2O],[22] has two sets of tunnels with different sizes (described using the $P\bar{1}$ space group). The structure can be conveniently described in terms of iron–iron distances. Along the small diagonal of the largest lozenge (c-axis), the distances between two nearest

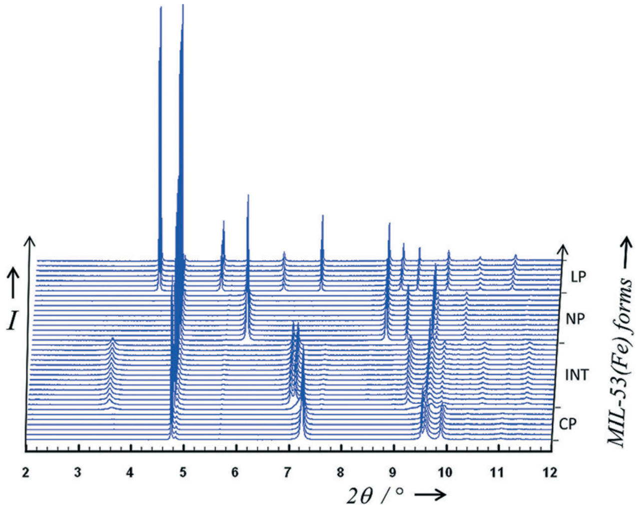

Fig. 3 Adsorption of CO_2 on MIL-53(Fe) followed by X-ray powder diffraction. Four different phases can be identified depending on the pressure and/or temperature (anhydrous CP, INT, NP and LP forms).

iron(III) cations increase significantly from Fe_2–Fe_2 = 7.762 Å and Fe_1–Fe_1 = 7.499 Å in MIL-53(Fe)_int to Fe_2–Fe_2 = 8.127 Å and Fe_1–Fe_1 = 8.109 Å in the(INT) form, while the in the smallest lozenge, there are nearly no changes (Fe_2–Fe_2 = 5.723 Å and Fe_1–Fe_1 = 5.993 Å in MIL-53(Fe)_int to Fe_2–Fe_2 = 5.847 Å and Fe_1–Fe_1 = 5.846 Å in the(INT) form). It is obvious that the smallest tunnels remain empty during the first stage of CO_2 uptake, and that the guests can only lie in half of the channels, the largest ones (see Fig. 4). The difference Fourier map calculations reveal unambiguously the exact position of the CO_2 molecule located at the centre of the largest pores, whereas no electron density was observed in the smallest ones. Analysis of the position of the CO_2 molecules led us to understand the nature of the host–guest and guest–guest interactions. Contrary to what has been observed in MIL-53(Sc)-int in which the CO_2 molecules are aligned with the long diagonal of the rhombic cross section of the channel,[13] in our case the CO_2 molecules are stacked along the *a*-axis in such a way that they are (i) almost parallel to each other and (ii) nearly parallel to the inorganic chains. However, a small tilt of the CO_2 molecule with the inorganic chain is observed in order to favour interactions between the oxygen atom (O_3) of the guest molecule and the OH/F group (O_1) of the two opposite inorganic chains in the direction of the small diagonal of the lozenge with a distance $d(O_3\cdots O_1)$ = 2.83(2) Å. All hydroxyl groups of the filled tunnels are then involved in hydrogen bonding with the guest molecule but there is no interaction between the CO_2 molecules themselves $d(O_3\cdots O_3)$ = 4.793(3) Å.

The (NP) form crystallises in a monoclinic unit cell (see Table 1). The crystallographic asymmetric unit contains one independent iron atom (on a symmetry centre), one OH/F group (on the twofold axis) and one carboxylate moiety (also on a symmetry centre). The disordered CO_2 molecule was localised on general position with occupancy of 0.313(2). Contrary to the (INT) form, all of the tunnels are equivalent and now filled by the CO_2 guest molecule at the centre of the pores. Along the small diagonal of the largest lozenge (*b*-axis), the distance between two nearest iron(III) cations is Fe–Fe = 8.251 Å in the (NP) form (see Fig. 5). This distance is close to that previously observed in the largest filled tunnel in the (INT) form and much larger than the one seen in MIL-53(Fe)[H_2O] (Fe–Fe = 7.643 Å) as expected taking into account the kinetic diameter of both different guest molecules.[23] In this (NP) form, the CO_2 molecules are closely aligned with the long diagonal of the rhombic cross section of the channels and stacked along the *c*-axis in such a way that they are (i) almost parallel to each other and (ii) nearly perpendicular to the inorganic chains. This stacking seen in the (NP) form is in closed agreement with the one found from *ab initio* molecular dynamics simulations for MIL-53(Sc)-int, even if only half the pores were filled by CO_2 in that case.[13] Half of the OH/F groups (O_1) now interact with only one oxygen atom of the CO_2 guest molecule (O_3) with a distance $d(O_3\cdots O_1)$ = 2.923(4) Å. Like in the (INT) form, no guest–guest

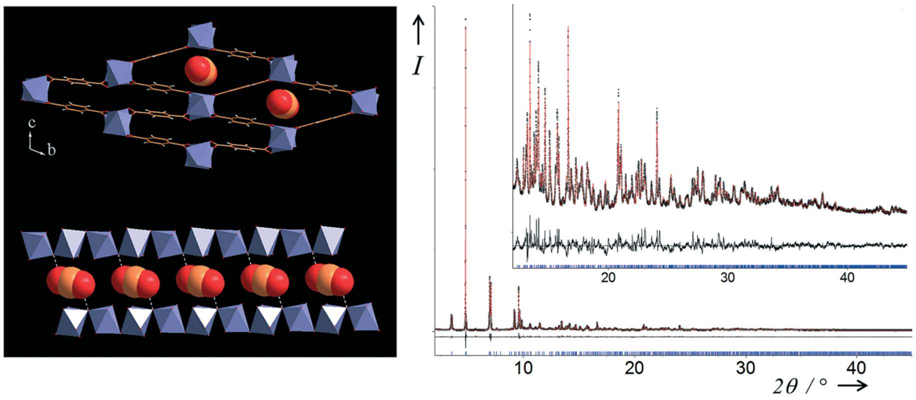

Fig. 4 Two views of the structure of MIL-53(Fe)[$0.22CO_2$] (top left) in the *bc* plane showing stacked CO_2 molecules within the largest lozenge-shaped channels and (bottom left) view of the filled single channel in the almost perpendicular direction. Final Rietveld plot (right) for MIL-53(Fe)[$0.22CO_2$] from X-ray powder diffraction data measured at room temperature and 2 bar. Black points correspond to experimental data and the red line to the calculated ones; the black line is the difference curve and the tickmarks indicate Bragg peak positions.

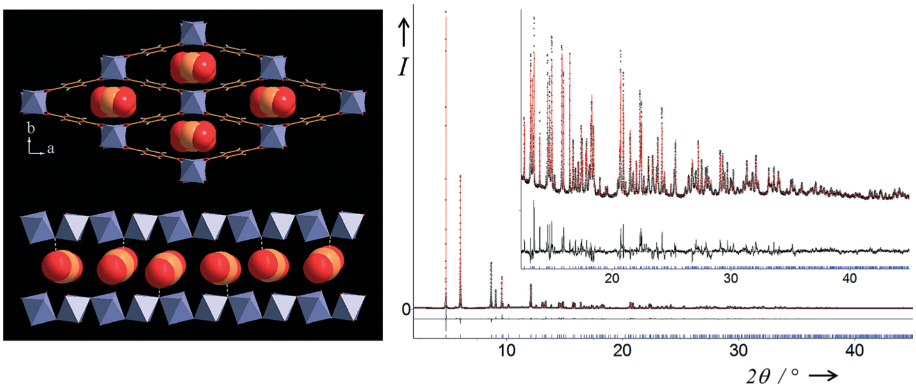

Fig. 5 Two views of the structure of MIL-53(Fe)[0.63CO_2] (top left) in the *ab* plane showing stacked CO_2 molecules within all the lozenge-shaped channels and (bottom left) view of a single channel in the almost perpendicular direction. Final Rietveld plot (right) for MIL-53(Fe)[0.63CO_2] from X-ray powder diffraction data measured at RT and 10 bar. Legend as Fig. 4.

interactions can be identified with the closest distance $d(O_3\cdots O_3) = 4.659(1)$ Å.

The (LP) form crystallises in an orthorhombic unit cell (see Table 1). The crystallographic asymmetric unit contains one independent iron atom sited on the 4*d* Wyckoff position, one OH/F group (4*e*) and one carboxylate moiety (centred on 4*b*) and two disordered independent CO_2 molecules, the first one being centered on 8*h* (occupancy of 0.5) and the second one on general position [occupancy of 0.430(2)]. In that form, a huge increase of the small diagonal of the lozenge has been observed (Fe–Fe = 13.638 Å) suggesting drastic changes in the amount of CO_2 inside the pores in comparison with the two previous forms (see Fig. 6). This is reminiscent of both the structure of the superhydrated chromium form MIL-53(Cr)[6.2H_2O] (Fe–Fe = 15.245 Å)[24] and the structure of the MIL-53(Fe)[2,6-lutidine,H_2O] (Fe–Fe = 14.392 Å).[14] In the (LP) form, the two CO_2 molecules are no longer localised at the centre of the pores: the first type (named **A**) are now located either side of the large diagonal of the lozenge, while the second type (named **B**) are sited either side of the small diagonal, which leads to a split of all CO_2 sites. This can explain the n_{max} value (see Table 1) corresponding to the maximum quantity of CO_2 able to fit in each MIL-53(Fe)[nCO_2]. Indeed, knowing that the n_{max} values for the two corresponding (INT) and (NP) forms are 0.25 and 1 respectively, and taking into account that (i) all channels are filled and (ii) all CO_2 sites are split in the (LP) form, this leads to a n_{max} value of 3 ($2 \times 2 \times 0.25 + 2 \times 1$) for this latter form. The **A** molecules adopt almost the same orientation as in the (INT) form: they are stacked along the inorganic chains (*c*-axis) and parallel to these chains, and they are strictly parallel to each other. The **B** molecules adopt almost the same orientation as in the (NP) form: they are mostly aligned with the long diagonal of the rhombic cross section of the channel and stacked along the *c*-axis in such a way that (i) the torsion angle between two adjacent CO_2 molecules is about 30° and that they are (ii)

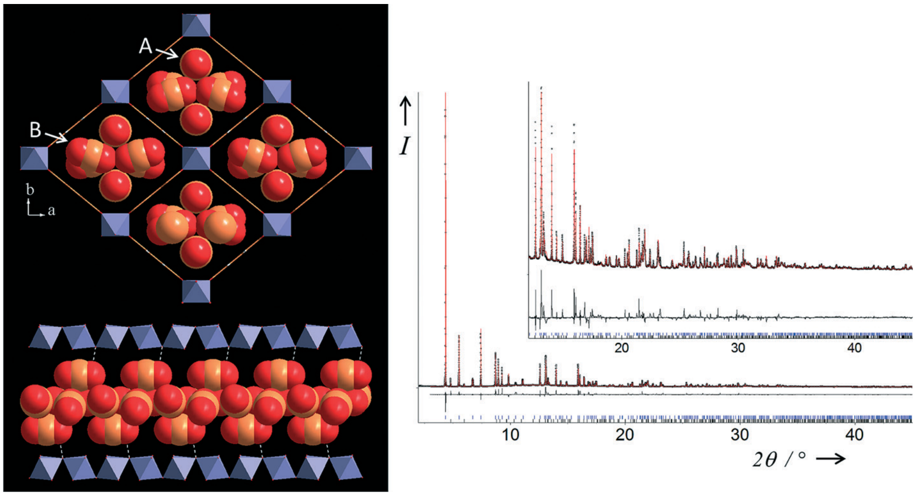

Fig. 6 Two views of the structure of MIL-53(Fe)[2.72CO_2] (top left) in the *ab* plane showing stacked CO_2 molecules (two types, labelled **A** and **B**) within all the lozenge-shaped channels and (bottom left) view of a single channel in the almost perpendicular direction. Final Rietveld plot (right) for MIL-53(Fe)[2.72CO_2] from X-ray powder diffraction data measured at 220 K and 10 bar. Legend as Fig. 4. The blue tickmarks (upper) indicate Bragg peak positions of the LP form (97.44(4)% weight) and the black ones (lower) those of the NP form observed as an impurity (2.56(4)% weight).

nearly perpendicular to the inorganic chains. Contrary to the (INT) form where each CO_2 molecule is sharing two OH/F groups of two adjacent inorganic chains, all the OH/F groups (O_1) are now involved in hydrogen bonding but with only one oxygen atom of the **A** molecule (O_2) with a distance $d(O_2\cdots O_1) = 3.014(6)$ Å. There is no interaction between the **A** molecules themselves $d(O_2\cdots O_3) = 4.578(1)$ Å. However, the carbon atom of this **A** molecule is in close contact with one oxygen atom of two **B** molecules [$d(C_2\cdots O_5) = 3.239(1)$ Å and $d(C_2\cdots O_5) = 3.200(1)$ Å)]. This short contact agrees well with the closest distance between two adjacent molecules found in the solid CO_2 structure, where $d(C\cdots O) = 3.107(1)$ Å even if the orientation is different: in the solid, CO_2 molecules arrange themselves in successive planes but pointing in the opposite direction relative to each other.[25] Therefore, the neighboring **B** molecules are closely packed along the long diagonal of the lozenge-shaped tunnels with some evidence of guest–guest interaction.

4. Conclusions

We have determined accurate information regarding the location of adsorbent molecules in one of the prototypical flexible metal–organic frameworks. Although studies of CO_2 adsorption in various forms of MIL-53 have previously been reported and the location of the guest molecules determined from simulation, this study is the only one to locate accurately from powder diffraction the positions of the guest molecules at various stages of the multi-step adsorption process. The $n_{\max}$ values for the two corresponding (INT) and (NP) forms are in good agreement with the CO_2 uptake seen on the two plateau regions. Like the Sc^{3+} analogue of the material (one of the rare cases where guest location has been reported),[13] the Fe^{3+} form takes up CO_2 at low pressures to give a structure in which alternate channels are filled, but in order to favour interactions between the oxygen atom of the guest molecule and the framework OH/F groups the CO_2 molecules are orientated differently. At higher pressure all pores are occupied and filled by the CO_2 guest molecule at their centres: again the predominant interaction appears to be with the framework OH/F groups rather than guest–guest interactions. At the highest pressure applied the CO_2 molecules are no longer found at the centre of the pores: one type is located either side of the large diagonal of the lozenge, while a second type is sited either side of the small diagonal. Here guest–guest interactions, similar to seen in solid CO_2 are also observed. In this form the MIL-53 structure is fully open and the CO_2 capacity is maximised.

Acknowledgements

We thank the ESRF for beamtime on ID31. We are grateful to Dr Andy Fitch and Dr Adrian Hill of the ESRF for their assistance with running the experiments on ID31. Some of the authors would like to acknowledge the financial support of the European Community STREP project "DeSANNS" (no. FP6-SES6-020133).

References

1 *Functional Metal-Organic Frameworks: Gas Storage, Separation and Catalysis*, ed. M. Schröder, Springer-Verlag Berlin Heidelberg, 2010; *Metal-Organic Frameworks: Applications from Catalysis to Gas Storage, Separation and Catalysis*, ed. D. Farrusseng, Wiley-VCH Verlag, Weinheim, 2011; S. T. Meek, J. A. Greathouse and M. D. Allendorf, *Adv. Mater.*, 2011, **23**, 249; H. Furukawa, K. E. Cordova, M. O'Keeffe and O. M. Yaghi, *Science*, 2013, **341**, 974.

2 J.-R. Li, Y. Ma, M. C. McCarthy, J. Sculley, J. Yu, H.-K. Jeong, P. B. Balbuena and H.-C. Zhou, *Coord. Chem. Rev.*, 2011, **255**, 1791; Y. S. Bae and R. Q. Snurr, *Angew. Chem., Int. Ed.*, 2011, **50**, 11586; J. Liu, P. K. Thallapally, B. P. McGrail, D. R. Brown and J. Liu, *Chem. Soc. Rev.*, 2012, **41**, 2308; Y. Liu, Z. U. Wang and H.-C. Zhou, *Greenhouse Gases: Sci. Technol.*, 2012, **2**, 239; B. Li, H. L. Wang and B. L. Chen, *Chem. – Asian J.*, 2014, **9**, 1474; Z. J. Zhang, Y. G. Zhao, Q. H. Gong, Z. Li and J. Li, *Chem. Commun.*, 2013, **49**, 653.

3 D. Britt, H. Furukawa, B. Wang, T. G. Glover and O. M. Yaghi, *Proc. Natl. Acad. Sci. U. S. A.*, 2009, **106**, 20637.

4 H. Wu, Y. S. Chua, V. Krungleviciute, M. Tyagi, P. Chen, T. Yildirim and W. Zhou, *J. Am. Chem. Soc.*, 2013, **135**, 10525.

5 C. H. Lau, R. Babarao and M. R. Hill, *Chem. Commun.*, 2013, **49**, 3634.

6 J. W. Yoon, S. H. Jhung, Y. K. Hwang, S. M. Humphrey, P. T. Wood and J. S. Chang, *Adv. Mater.*, 2007, **19**, 1830.

7 S. Kitagawa and K. Uemura, *Chem. Soc. Rev.*, 2005, **34**, 109; S. Bureekaew, S. Shimomura and S. Kitagawa, *Sci. Technol. Adv. Mater.*, 2008, 9; A. Schneemann, V. Bon, I. Schwedler, I. Senkovska, S. Kaskel and R. A. Fischer, *Chem. Soc. Rev.*, 2014, **43**, 6062.

8 G. Férey and C. Serre, *Chem. Soc. Rev.*, 2009, **38**, 1380.

9 F. Millange, C. Serre and G. Férey, *Chem. Commun.*, 2002, 822.

10 F. Nouar, T. Devic, H. Chevreau, N. Guillou, E. Gibson, G. Clet, M. Daturi, A. Vimont, J. M. Grenèche, M. I. Breeze, R. I. Walton, P. L. Llewellyn and C. Serre, *Chem. Commun.*, 2012, **48**, 10237; M. I. Breeze, G. Clet, B. C. Campo, A. Vimont, M. Daturi, J.-M. Grenèche, A. J. Dent, F. Millange and R. I. Walton, *Inorg. Chem.*, 2013, **52**, 8171.

11 T. Devic, F. Salles, S. Bourrelly, B. Moulin, G. Maurin, P. Horcajada, C. Serre, A. Vimont, J.-C. Lavalley, H. Leclerc, G. Clet, M. Daturi, P. L. Llewellyn, Y. Filinchuk and G. Férey, *J. Mater. Chem.*, 2012, **22**, 10266.

12 S. Couck, E. Gobechiya, C. E. A. Kirschhock, P. Serra-Crespo, J. Juan-Alcaniz, A. M. Joaristi, E. Stavitski, J. Gascon, F. Kapteijn, G. V. Baron and J. F. M. Denayer, *ChemSusChem*, 2012, **5**, 740; L. Chen, J. P. S. Mowat, D. Fairen-Jimenez, C. A. Morrison, S. P. Thompson, P. A. Wright and T. Düren, *J. Am. Chem. Soc.*, 2013, **135**, 15763.

13 J. P. S. Mowat, V. R. Seymour, J. M. Griffin, S. P. Thompson, A. M. Z. Slawin, D. Fairen-Jimenez, T. Düren, S. E. Ashbrook and P. A. Wright, *Dalton Trans.*, 2012, **41**, 3937.

14 F. Millange, N. Guillou, M. E. Medina, G. Férey, A. Carlin-Sinclair, K. M. Golden and R. I. Walton, *Chem. Mater.*, 2010, **22**, 4237.

15 P. L. Llewellyn, P. Horcajada, G. Maurin, T. Devic, N. Rosenbach, S. Bourrelly, C. Serre, D. Vincent, S. Loera-Serna, Y. Filinchuk and G. Férey, *J. Am. Chem. Soc.*, 2009, **131**, 13002.

16 *Topas V4.2: General Profile and Structure Analysis Software for Powder Diffraction Data*, Bruker AXS Ltd, 2008.

17 G. De Weireld, M. Frere and R. Jadot, *Meas. Sci. Technol.*, 1999, **10**, 117.

18 A. Ghoufi, L. Gaberova, J. Rouquerol, D. Vincent, P. L. Llewellyn and G. Maurin, *Microporous Mesoporous Mater.*, 2009, **119**, 117.

19 P. L. Llewellyn and G. Maurin, *C. R. Chim.*, 2005, **8**, 283.

20 S. Bourrelly, P. L. Llewellyn, C. Serre, F. Millange, T. Loiseau and G. Férey, *J. Am. Chem. Soc.*, 2005, **127**, 13519.

21 N. A. Ramsahye, G. Maurin, S. Bourrelly, P. L. Llewellyn, C. Serre, T. Loiseau, T. Devic and G. Férey, *J. Phys. Chem. C*, 2008, **112**, 514.

22 F. Millange, N. Guillou, R. I. Walton, J.-M. Grenèche, I. Margiolaki and G. Férey, *Chem. Commun.*, 2008, 4732.

23 N. Guillou, R. I. Walton and F. Millange, *Z. Kristallogr. - Cryst. Mater.*, 2010, **225**, 552.

24 N. Guillou, F. Millange and R. I. Walton, *Chem. Commun.*, 2011, **47**, 713.

25 A. Simon and K. Peters, *Acta Crystallogr., Sect. B: Struct. Crystallogr. Cryst. Chem.*, 1980, **36**, 2750.